

Journal of Solar Energy Research (JSER)

Journal homepage: www.jser.ut.ac.ir



Experimental Analysis of Drying Performance in ETC-Assisted Solar Dryers: Influence of Collector Count and Soil Particle Size

Vinaya,b,*, N.K. Singhc, Avadhesh Yadavd

- ^aSchool of Renewable Energy and Efficiency, National Institute of Technology, Kurukshetra, Haryana 136119, India
- ^bDepartment of Mechanical Engineering, Manav Rachna International Institute of Research and studies, Haryana 121004 India
- ^cDepartment of Mechanical Engineering, National Institute of Technology, Kurukshetra, Haryana 136119, India ^dSolar Thermal Division, National Institute of Solar Energy, Gurugram, Haryana 122003, India

ARTICLE INFO

Article Type:

Research Article

Received:2025.09.29 Accepted in revised form: 2025.11.22

Keywords:

Agricultural drying; Drying efficiency; Drying rate; Evacuated tube collectors (ETC); Passive solar dryer; Sand-based thermal storage;

ABSTRACT

Solar drying provides a sustainable substitute for traditional fuel-based preservation techniques by harnessing renewable thermal energy. This study investigates the impact of the number of evacuated tube collectors (ETC), ranging from 1 to 3, and the size of sand particles—fine-grained (FGS), medium-grained (MGS), and coarsegrained (CGS)—on the efficacy of a solar dryer that incorporates sand-based thermal storage. Experiments were performed under three ETC configurations utilizing grated carrot samples, with drying performance assessed based on drying rate (0.57-0.93 g/min) and drying efficiency (up to 70.7%). The findings indicated that augmenting the quantity of ETCs improved the drying rate, achieving a peak of 0.93 g/min with FGS in the three-ETC configuration, succeeded by MGS and CGS. Fine sand exhibited enhanced heat conductivity, facilitating expedited moisture removal, whereas medium and coarse grains provided more consistent drying in subsequent phases. Nonetheless, drying efficiency diminished with increased ETC counts, declining from 70.7% (FGS-1 ETC) to approximately 20.7% (FGS-3 ETC). The results highlight the compromise between attaining increased drying rates and preserving thermal efficiency, offering guidance for the optimization of solar dryer designs that integrate thermal energy storage materials.

Cite this article: a, V., Singh, N. and Yadav, A. (2025). Experimental Analysis of Drying Performance in ETC-Assisted Solar Dryers: Influence of Collector Count and Soil Particle Size. Journal of Solar Energy Research, 10(3), 2559-2574. doi: 10.22059/jser.2025.403175.1643

DOI: 10.22059/jser.2025.403175.1643



©The Author(s). Publisher: University of Tehran Press.

^{*}Corresponding Author Email:exresearchscholar@gmail.com

1. Introduction

The removal of moisture of agricultural products is among the most ancient preservation techniques; yet, its advancement via solar energy has markedly revolutionized the sector. Solar dryers offer numerous benefits over open-sun drying, including reduced pollution, improved nutrient preservation, and accelerated drying times. In recent years, researchers have developed many technologies that improve drying efficiency while reducing dependence on fossil fuels [1]. A significant breakthrough is the hybrid photovoltaic-thermal system, which combines power generation with heat collection to facilitate continuous drying processes. These designs have exhibited thermal efficiency above 50% and have been utilized for crops such as grapes and vegetables [2]. Additional improvements encompass photovoltaic-thermoelectric (PVT-TEG) systems, which maintain steady operation by concurrently gathering electrical and thermal energy [3]. The utilization of phase change materials (PCMs) has emerged as a significant method in solar drying research. By absorbing and releasing heat at regulated temperatures, phase change materials mitigate temperature variations within the drying chamber and prolong drying into the evening hours. Research on the drying of mango, banana, and tomato indicates that PCM-assisted methods yield more uniform moisture extraction and diminish the likelihood of spoiling [4]. Comparative studies demonstrate that the utilization of PCMs enhances product quality and system sustainability [5]. In addition to storage integration, system geometry has been essential in enhancing performance. Finned and double-pass air collectors have been evaluated for peppermint desiccation, yielding enhanced heat transmission and optimized energy utilization [6]. Furthermore, spiral-shaped solar dryers integrated storage medium exhibited stable temperature profiles and advantageous drying rates for tomato slices [7]. Evacuated tube collectors have garnered interest due to their exceptional capacity to absorb diffuse radiation, which is especially advantageous in regions with sporadic sunlight [8],[9]. Investigations have also progressed into specialized chamber arrangements. Transforming a greenhouse into a solar dryer established an atmosphere conducive to both plant cultivation and produce drying, hence optimizing land utilization [10]. Other experiments with baffled chambers in mango slice dryers improved airflow distribution and accelerated drying [11]. By refining airflow, chamber temperature, and structural design, these

systems reduced energy losses and achieved higher throughput with minimal additional cost [12]. Beyond physical design, solar drying has seen growing adoption of digital tools. IoT-enabled monitoring systems have been introduced to provide real-time adjustments in airflow and chamber temperature, ensuring better control of drying conditions [13],[14]. Smart control platforms enable farmers to reduce over-drying and energy waste, while still achieving microbial safety standards[15]. The applications of solar drying are remarkably diverse. Hybrid systems have been tested for fruits such as raspberries, peanuts, and chilies, as well as for leafy vegetables and herbs [16]. Each application shows consistent superiority over open-sun drying in terms of nutrient preservation, retention of color, and reduction of microbial contamination [17]. For example, experiments on raspberry drying in a pulse-spouted microwave-assisted freeze dryer highlighted the advantages of controlled thermal environments for delicate fruits [18]. Similarly, the drying of herbs such as peppermint demonstrated the value of forced-convection dryers in maintaining essential oil composition [19]. Kinetic modelling continues to support design and optimization. Models such as Page, Henderson-Pabis, and logarithmic equations are regularly applied to describe moisture removal behaviour across different products [20]. These models allow predictive assessment of drying time, rate, and efficiency, thus guiding the selection of optimal configurations for particular crops [21]. Furthermore, techno-economic assessments highlight the practicality of solar dryers, with reported payback periods ranging from two to five vears depending on design complexity and crop type [22]. Studies consistently confirm substantial reductions in carbon emissions compared to traditional fossil-fuel dryers, positioning solar drying as a vital component of sustainable agriculture [23]. Ahmed Kadhim Hussein [24] highlighted nanotechnology as a transformative solution to 21stcentury energy challenges. His review comprehensively examined theoretical and experimental research nanotechnology on applications across renewable energy systems, biomass, including wind, solar, hydrogen, geothermal, and tidal energy. The findings revealed that nanomaterials significantly enhanced the efficiency, cost-effectiveness, and environmental sustainability of renewable energy technologies. Nanotechnology contributed to advanced energy conversion, storage, and green material design while supporting cleaner energy production and reducing

fossil fuel dependence. It also played a crucial role in hydrogen energy and biofuel development. However, the study emphasized the need for further research, particularly in geothermal, wind, and tidal applications, where existing literature remained limited. Ahmed Kadhim Hussein et al. [25] provided a comprehensive review of recent advancements in applying nanotechnology to direct absorption solar collectors (DASCs). They analyzed theoretical, numerical, and experimental research to evaluate the role of nanofluids in enhancing solar energy absorption and conversion efficiency. The findings indicated that nanofluids significantly improved the thermal performance of DASCs through superior heat transfer and light absorption characteristics. The review highlighted the importance of optimizing nanoparticle dispersion, shape, and volume fraction to maximize efficiency. Additionally, it emphasized the need for future research focused on developing cost-effective, non-toxic nanoparticles and reliable energy transport mechanisms. Environmental and economic assessments were also recommended to ensure the sustainable implementation of nanofluidbased solar collector systems. Ahmed Kadhim Hussein [26] provided a thorough review of recent developments in the application of nanotechnology across various solar collector types, including flat plate, direct absorption, parabolic trough, wavy, heat pipe, and hybrid systems. The review compiled theoretical, numerical, and experimental studies to provide an extensive understanding of how nanofluids enhanced the thermal efficiency and optical performance of solar collectors. The results revealed that nanoparticle dispersion, size, shape, and volume fraction significantly influenced system performance, with carbon nano horns identified as particularly promising materials. The study also highlighted challenges such as particle sedimentation, agglomeration, and stability, emphasizing the need for further research on hybrid nanofluids, environmentally friendly materials, and cost-effective designs. Overall, nanotechnology offered great potential to revolutionize solar collector efficiency, reliability, and sustainability in future energy systems. Hussein et al. [27] presented a comprehensive review of recent advancements in the application of nanofluids in heat pipe solar collectors (HPCs). It summarized theoretical, numerical, and experimental studies to evaluate how nanotechnology enhanced the performance of these systems. The findings indicated that nanofluids significantly improved the heat transfer efficiency and solar absorption capability of HPCs. Optimal nanoparticle dispersion, size, and volume fraction

were found to be crucial for achieving maximum efficiency. The study emphasized the potential of carbon nano horns (CNHs) due to their large surface area and superior optical properties. It also highlighted challenges such as particle agglomeration, migration, and stability, along with the need for low-cost, non-toxic nanoparticles. Future research was suggested to explore hybrid nanofluids, investigate optical effects beyond thermal conductivity, and assess environmental and economic aspects to ensure sustainable HPC development. Nasim Hashemian and Alireza Noorpoor [28] proposed a novel multi-generation hybrid energy system that integrated solar and wind resources to produce power, heating, cooling, hvdrogen. and ammonia. The configuration combined a wind turbine with a steam Rankine cycle for electricity generation, a dual-effect absorption cooling system for cooling demands, and a heat exchanger for thermal energy recovery. Furthermore. hvdrogen and ammonia generated via a proton exchange membrane electrolyzer and a reactor, respectively. The system produced notable outputs: 44.8 MW of power, 20.64 MW of heat, 123.9 MW of cooling, 263.1 kg/h of hydrogen, and 106.48 kg/h of ammonia. Thermoeconomic-environmental analysis indicated energy efficiency of 83.65% and exergy efficiency of 17.97%, with a total product cost rate of \$1.44 per second. The optimization results demonstrated that the parabolic trough solar collector was responsible for the majority of exergy destruction, accounting for 57%, with an ambient temperature of 35°C yielding optimal performance. Hashemian and Noorpoor [29] developed a biomass-solar hybrid multi-generation system capable of concurrently generating electricity, heating, cooling, hydrogen, and potable water. The system incorporated a steam Rankine cycle, a double-effect absorption chiller, a proton exchange membrane electrolyzer, a multieffect desalination unit, and a parabolic trough solar collector. Thermodynamic, exergy-economic, and exergy-environmental analyses were conducted to evaluate system feasibility, cost flow, environmental performance. The findings indicated energy and exergy efficiencies of 82.4% and 14%, respectively, alongside a total product cost rate of \$0.84 per second and an exergy-environmental impact factor of 0.15. The system generated 26.3 MW of power, 137.3 MW of cooling, 21.4 MW of heating, 72 kg/h of hydrogen, and 3927 m³/h of potable water, utilizing 6.2 ton/h of bagasse and a solar collector area of 188,000 m². The optimization via a genetic algorithm resulted in an enhanced

exergy efficiency of 16.53% and a decreased cost rate of \$0.71/s, thereby validating the system's significant thermodynamic and economic potential for sustainable energy generation.

The current research indicates that advancements in hybridization, energy storage, collector design, chamber configuration, and intelligent monitoring have synergistically enhanced solar drying into a dependable and sustainable method. advancements highlight its promise environmentally sustainable method for food preservation. This study expands on previous research by examining the drying rate and efficiency of evacuated tube collectors combined with soilbased thermal storage, in accordance contemporary worldwide trends in sustainable energy applications. This study examines innovative elements, specifically traditional passive solar dryers that depend exclusively on natural convection. The suggested system incorporates evacuated tube collectors (ETCs) to warm incoming air, hence improving thermal availability and drying efficiency without requiring external energy input. The work presents the novel application of stone dust (sand) with varying particle sizes (≤300 µm, ~600 µm, and ~1.18 mm) incorporated in copper trays as an economical and sustainable heat storage medium, offering a viable substitute for costly phase change materials (PCMs). This research provides a comprehensive evaluation of moisture kineticsincluding wet basis moisture content (MCwb), dry basis moisture content (MC_{db}), and moisture ratio (MR)—for grated carrot across different ETC configurations and sand fractions, rather than restricting the analysis to temperature or energy efficiency. The work distinctly delineates the interactive effects of collector quantity and sand particle dimensions on drying efficacy, thereby providing a scientific foundation for designing efficient, material-adaptive, and economically viable solar drying systems tailored for decentralized agricultural use.

2. Materials and Methods

2.1 Experimental System Design

The experimental dryer was designed as a passive solar drying system that combined evacuated tube collectors (ETCs) with sand-based thermal storage. The main drying chamber was fabricated from wood and covered with transparent acrylic sheets. This cover reduced convective heat losses while allowing solar radiation to penetrate the chamber, as shown in

Figure 4. A copper tray was placed inside the chamber, beneath which sand was filled, chosen for its local availability, low cost, and stable thermal behaviour. Each chamber was packed with 10 kg of sand, as illustrated in Figure 1. Three distinct sand particle sizes were tested: fine-grained sand (FGS ≤ 300 µm), medium-grained sand (MGS \approx 600 µm), and coarse-grained sand (CGS ≈ 1.18 mm), shown in Figure 2. In operation, heat transfer followed a stepwise process. Solar radiation was first absorbed by the evacuated tubes, which heated the working fluid inside the heat pipes. The heat was then conducted to the hot bulb region of the heat pipe that extended into the drying chamber. This hot bulb transferred heat directly to the surrounding sand bed. The sand acted as both a heat transfer medium and a thermal storage unit: during peak radiation hours, it quickly heated up, and when solar intensity decreased, it released the stored heat gradually. This ensured that the drying process could continue even under fluctuating or low solar radiation conditions. The grated carrot samples (200 g per run) were spread evenly over the copper drying tray (Figure 5) placed above the sand bed. Heat conducted through the sand and copper tray elevated the product temperature, enhancing moisture removal. This design provided direct heating during sunshine and sustained drying during off-peak periods, making the system both energy-efficient and practical for rural applications. Collector augmentation was achieved by configuring one, two, or three ETCs, inclined at site latitude to maximize solar absorption.

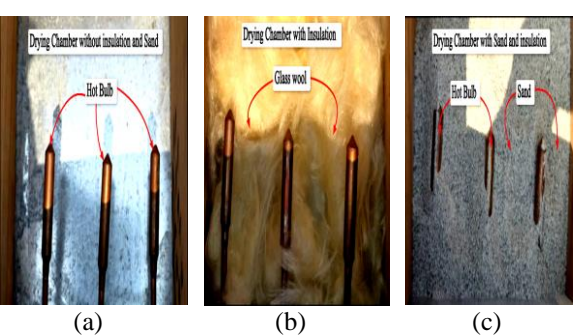


Figure 1. Drying chambers under different configurations - (a) without insulation and sand, (b) with glass wool insulation, and (c) with sand and insulation

Studies have shown that evacuated tubes outperform flat-plate collectors in harnessing diffuse radiation, making them well-suited for Indian climates. The schematic arrangement is shown in Figure 3, while the fabricated system is presented in Figure 6 with a grated carrot on a drying tray. Previous researchers have confirmed that hybrid designs combining thermal storage with ETCs yield superior drying performance.



Figure 2. Classification of dust fractions: (a) Fine $(\le300 \mu m)$, (b) Medium ($\sim600 \mu m$), and (c) Coarse

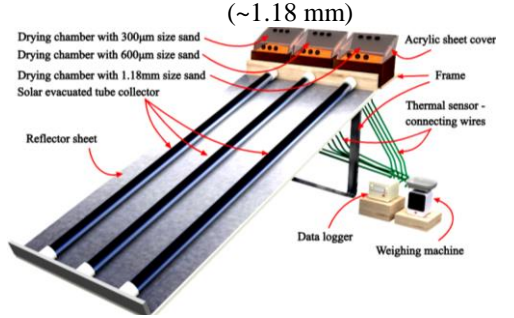


Figure 3. Schematic of the experimental setup used for passive solar drying

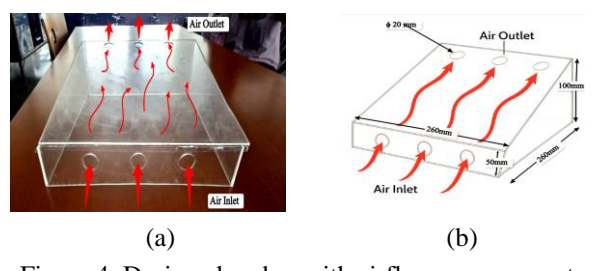


Figure 4. Drying chamber with airflow arrangement
— (a) fabricated acrylic chamber showing air inlet
and outlet flow, and (b) schematic representation
with dimensions and airflow path

2.2 Experimental Materials

Grated carrot was selected as the test product due to its high perishability and nutritional sensitivity. Each batch weighed 200 g and was spread evenly on perforated stainless-steel trays positioned above the heated sand bed. Such uniform distribution prevents clumping and ensures consistent exposure to airflow [30]. The decision to grate carrots instead of drying whole slices followed evidence that smaller particle sizes accelerate drying kinetics.

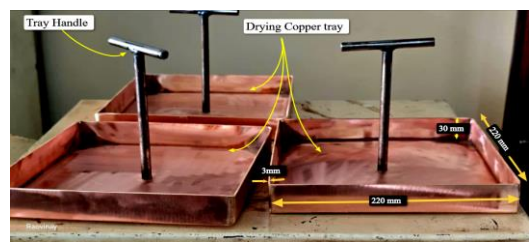


Figure 5. Drying copper tray

Carrot drying has been frequently used as a benchmark to evaluate the effectiveness of experimental dryers because of its rapid moisture loss and quality sensitivity [31]. The product loading arrangement is illustrated in Figure 5. By testing across FGS, MGS, and CGS beds, this study establishes comparative data on how sand particle size influences heat transfer during product drying. Carrot's response to drying further validates system efficiency as highlighted in earlier experimental works [32].

2.3 Instrumentation and Measurements

Solar radiation was monitored using a calibrated pyranometer, a standard practice in solar drying research [33]. Ambient temperature and humidity were measured with a thermos-hygrometer, while airflow was assessed by a digital anemometer [34]. Chamber and tray temperatures were recorded using K-type thermocouples, connected to a multi-channel data logger for accuracy. Mass reduction of the carrot load was measured with a digital balance accurate to ± 0.01 g, enabling calculation of drying rates at 30-minute intervals. Each measurement followed protocols consistent with prior work, ensuring repeatability and reliability. Previous emphasize that high-frequency studies collection allows precise modelling of drying kinetics [35]. Thus, the selected instruments provided sufficient resolution to capture transient variations in heat transfer and moisture removal across different sand beds, ETC configurations.

2.4 Experimental Procedure

Each test began with filling the copper tray with a uniform 25 mm layer of the selected sand fraction. The ETCs were then preheated for about 30 minutes to raise the bed temperature before loading the sample. After preheating, a 200 g grated carrot batch was placed on the tray, as shown in Figure 6. Data were collected from 10:00 to 18:00, coinciding with peak isolation hours. Measurements of solar intensity, ambient conditions, tray temperature, chamber temperature, and sample mass were taken every 30 minutes. The process continued until the carrot approached equilibrium moisture content. This systematic approach allowed direct comparison across FGS, MGS, and CGS configurations under one-, two-, and three-tube ETC arrangements. Flow sequencing of the experimental steps is summarized in Figure 6. The design ensured consistency between runs while reducing external variability [36].

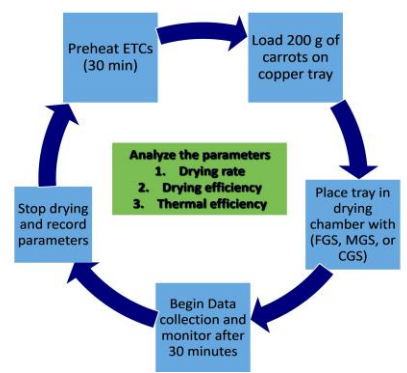


Figure 6. Graphical representation of the ETC-assisted solar dryer experimental process

2.5 Performance Evaluation

System performance was assessed using drying rate, drying efficiency, and thermal efficiency. Drying rate was calculated as the change in product mass per unit time (g/min), reflecting throughput. Drying efficiency was determined by comparing the energy utilized for evaporation against the total incident solar input [37]. Thermal efficiency quantifies the ratio of useful heat gain to absorbed solar radiation[38] . Evaluating these three indices together provides a balanced view of dryer performance. Previous research confirms that ETC augmentation increases drying rate but may lower efficiency due to thermal losses. Drying efficiency is particularly useful for comparing product-specific outcomes across studies[39].

Drying performance was evaluated using three key parameters:

• Drying Rate (g/min):

$$D_{R} = \Delta m / \Delta t \tag{1}$$

where Δm is the moisture removed (g) within the 30-minute interval Δt .

Drying Efficiency (%):

$$\eta_{d} = (m_w h_{fg}) / (I.A_c.t).100$$
 (2)

where m_w is the mass of water evaporated (kg), h_{fg} is the latent heat of vaporization (kJ/kg), I is the solar radiation intensity (W/m²), A_c is the collector area (m²), and t is the drying duration (s).

• Thermal Efficiency (%):

$$\eta_{th} = (Q_u) / (I.A_C). 100$$
 (3)

where Q_u is the useful heat gained (w), these parameters were computed separately for each ETC configuration and sand size to establish comparative performance.

2.6 Error Analysis

Experimental uncertainties primarily arose from measurement limitations, system variability, and environmental fluctuations. Mass measurements, used to determine drying rates, were taken using a digital balance with an accuracy of ± 0.1 g. For small moisture losses (5-10 g), this introduces a relative error of approximately 1-2%. Timing errors were minimal (±1 s) and had negligible influence over typical drying durations of 2-3 hours. Thermal measurements were performed using thermocouples or infrared sensors with an uncertainty of ±1°C, while solar radiation was monitored using a pyranometer (±2 W/m² accuracy). Variations in temperature and solar irradiance, particularly due to intermittent cloud cover, contributed to fluctuations calculated thermal efficiency. Additional variability stemmed from non-uniform sand packing density and particle size distribution, which affected thermal conductivity, as well as ambient factors such as wind speed and humidity that influenced convective losses.

2.7 Comparative Framework

To rank configurations, a decision matrix was applied, incorporating the drying rate [43]. Drying

rate was normalized and weighted equally, allowing the development of a composite performance score. The structure of the matrix is illustrated in Figure 7. Multi-criteria decision-making methods have been applied previously in energy research to identify optimal trade-offs between performance and sustainability [44]. In this study, the 2-ETC FGS system ranked highest, balancing high drying rate with moderate efficiency. This aligns with prior evidence that moderate system augmentation often delivers the most sustainable outcomes [45].

3. Results and Discussion

3.1 Drying Rate Analysis

3.1.1 Drying Rate under Single ETC for Different Sand Sizes

The drying profiles under a single ETC are shown in Figure 7. Among the three sand beds, fine-grained sand (FGS) delivered the fastest moisture removal, with a peak drying rate of ~0.50 g/min near midday. Medium-grained sand (MGS) followed closely, peaking at ~0.41 g/min, while coarse-grained sand (CGS) exhibited the lowest drying performance at ~0.37 g/min. The differences can be attributed to thermal conductivity: finer particles transfer heat more effectively to the drying tray, whereas larger grains retain heat but distribute it less efficiently. Thermal conductivity is a crucial property influencing heat transfer efficiency in these systems. Finer particles facilitate faster and more uniform moisture removal due to their ability to transfer heat more effectively, whereas larger grains tend to preserve heat within themselves but transfer it less efficiently, leading to different drying behaviors across sand sizes

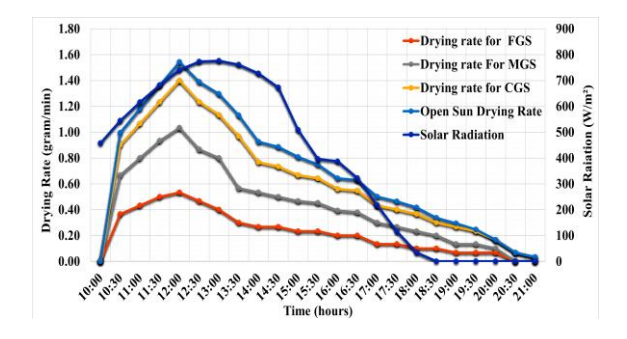


Figure 7. Drying Rate vs Time for Single ETC with FGS, MGS, and CGS

3.1.2 Drying Rate under Double ETC for Different Sand Sizes

The influence of increasing collectors to two ETCs is shown in Figure 8. Across all sand sizes, drying rates improved significantly, reflecting greater solar energy input. FGS reached a maximum of 0.63 g/min, outperforming MGS (0.54 g/min) and CGS (0.50 g/min). Importantly, the drying curves flattened in the late afternoon, showing that extra energy input sustained drying rates for longer compared to the single-ETC configuration.

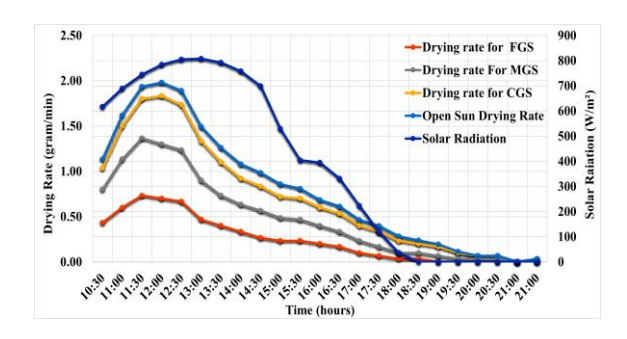


Figure 8. Drying Rate vs Time for Double ETC with FGS, MGS, and CGS

3.1.3 Drying Rate under Triple ETC for Different Sand Sizes

When the system was augmented to three ETCs, drying performance reached its highest level (Figure 9). The FGS–3 ETC system recorded the maximum drying rate of 0.77 g/min, establishing the strongest throughput. MGS and CGS followed with peaks of 0.69 g/min and 0.65 g/min, respectively. However, the efficiency of energy conversion decreased (to be discussed in Section 3.2). This shows that while triple ETCs deliver maximum drying speed, they also amplify thermal losses.

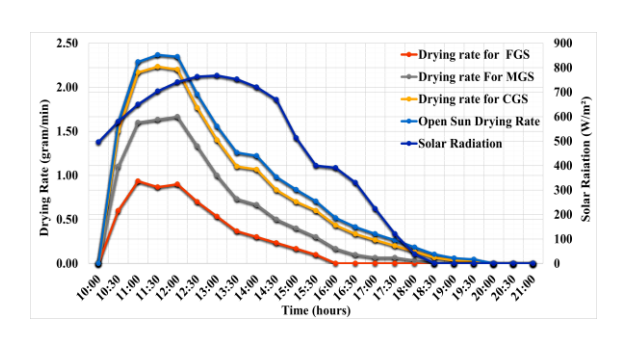


Figure 9. Drying Rate vs Time for Triple ETC with FGS, MGS, and CGS

3.1.4 Drying Rate of FGS under Different ETC Counts

The comparison of FGS drying under one, two, and three ETCs is illustrated in Figure 10. A clear upward trend was observed: 0.50 g/min (1 ETC), 0.63 g/min (2 ETCs), and 0.77 g/min (3 ETCs). The gain in drying capacity demonstrates the combined effect of particle fineness and higher solar capture.

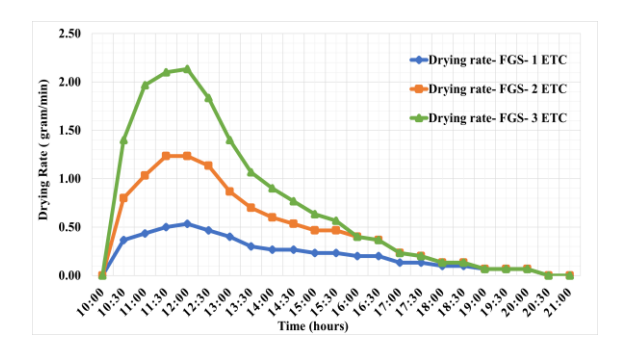


Figure 10. Drying Rate vs Time for FGS under 1, 2, and 3 ETCs

3.1.5 Drying Rate of MGS under Different ETC Counts

The response of MGS across one, two, and three ETCs is presented in Figure 11. The maximum drying rates progressed from 0.41 g/min (1 ETC) to 0.54 g/min (2 ETCs) and 0.69 g/min (3 ETCs). While MGS showed steady performance, its intermediate particle size meant that heat transfer was not as efficient as FGS.

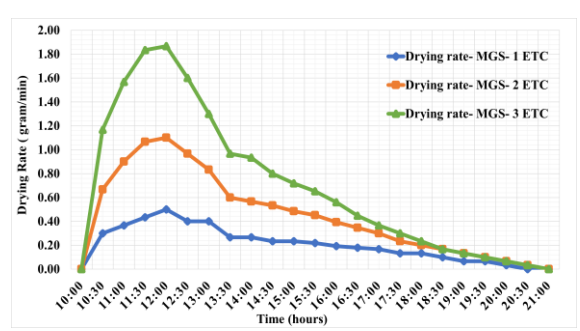


Figure 11. Drying Rate vs Time for MGS under 1, 2, and 3 ETCs

3.1.6 Drying Rate of CGS under Different ETC Counts

Finally, CGS drying rates under 1, 2, and 3 ETCs are shown in Figure 12. The maximum rates were 0.37

g/min (1 ETC), 0.50 g/min (2 ETCs), and 0.65 g/min (3 ETCs). While CGS delivered lower values compared to FGS and MGS, its performance improved consistently with collector augmentation, confirming that increased solar input compensates weaker heat transfer properties. improvement in CGS performance with increased collector count demonstrates that solar input acts as a compensatory factor. Higher solar energy availability enhances the overall thermal input, enabling less efficient heat transfer media like CGS to achieve higher drying rates and efficiencies, making system performance scalable with collector augmentation.

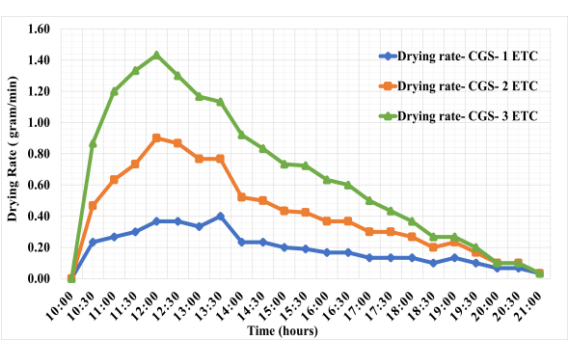


Figure 12. Drying Rate vs Time for CGS under 1, 2, and 3 ETCs

3.2 Drying Efficiency

Drying efficiency reflects the fraction of solar energy effectively used to remove moisture from the agricultural load, relative to the total solar input. In this study, drying efficiency was evaluated for finegrained sand (FGS), medium-grained sand (MGS), and coarse-grained sand (CGS) under single, double, triple evacuated tube collector (ETC) configurations. Measurements were recorded at 30minute intervals up to 17:30 h, coinciding with the solar window for efficient drying. At 1 ETC, drying efficiency peaked for FGS at ~20.7% around 17:30 h, while MGS and CGS displayed moderate values of ~20.7% and ~20.7%, respectively. Notably, efficiency trends showed an initial rise between 10:30 h and 12:00 h, followed by fluctuations linked to variable solar radiation, and later a sharp increase in the evening due to reduced input energy but sustained residual heating of the sand bed (Figure 13). During the morning hours, solar radiation intensity increases progressively as the sun ascends, enhancing the availability of incident energy on the collector surface. This rise in solar input results in a corresponding increase in the system's ability to convert incident radiation into useful thermal energy, leading to an initial improvement in thermal efficiency. As the sand bed and copper tray absorb greater amounts of heat, their temperature rises, which enhances conductive and convective heat transfer to the drying product, thereby accelerating moisture removal. However, as the day advances into the late afternoon and evening, the solar irradiance diminishes sharply, causing a reduction in the rate of thermal energy absorption and a consequent decline in drying efficiency.

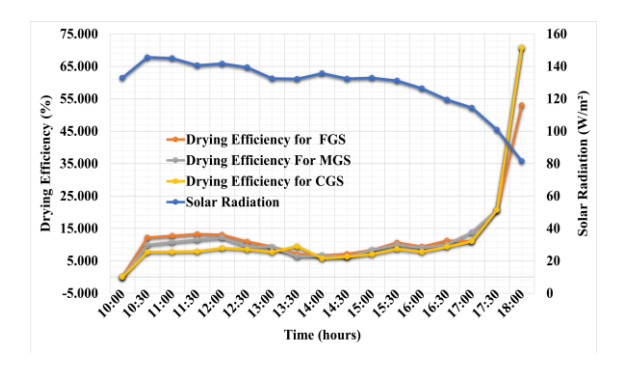


Figure 13. Drying Efficiency vs. Time for FGS, MGS, and CGS (1 ETC)

With 2 ETCs, the system exhibited more balanced profiles, where peak efficiencies of ~16.7% were achieved for MGS and CGS, while FGS remained slightly lower at ~8.3%. Compared to 1 ETC, double-tube operation reduced late-afternoon surges, stabilizing the energy use across the drying period (Figure 14). This indicates that distributing solar load over two tubes helps smooth fluctuations, improving the predictability of performance.

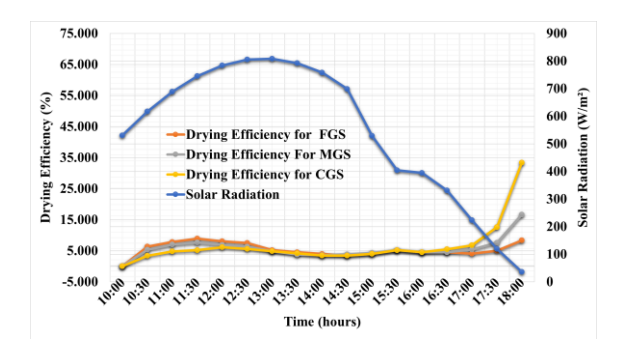


Figure 14. Drying Efficiency vs. Time for FGS, MGS, and CGS (2 ETCs)

Under 3 ETCs, overall drying efficiency values were lower, averaging 5–10% throughout the midday

period. Peak efficiencies for CGS (~15.8%) were only observed near sunset, while FGS efficiency declined sharply to nearly zero by 16:00 h (Figure 15). The reduction in efficiency is attributed to higher instantaneous thermal energy, causing increased convective and conductive losses.

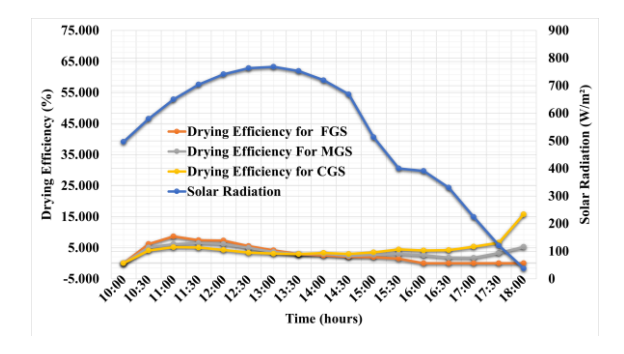


Figure 15. Drying Efficiency vs. Time for FGS, MGS, and CGS (3 ETCs)

A comparative view of drying efficiency by sand type (Figure 16) demonstrates that FGS consistently outperformed MGS and CGS in the 1 ETC configuration, whereas CGS became more favorable under higher ETC counts. This trade-off suggests that finer particles are better at storing and releasing heat at low-to-moderate inputs, while coarser media stabilize system behaviour under higher loads.

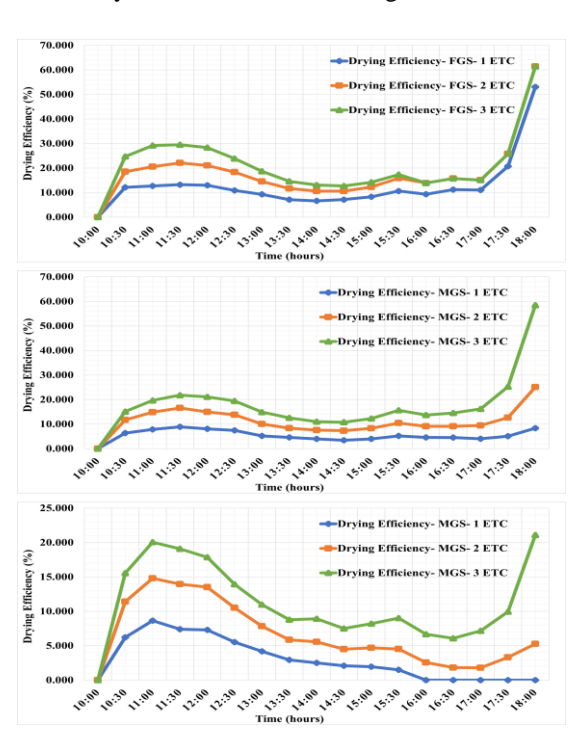


Figure 16. Variation of drying efficiency with time for different ETC configurations (1, 2, and 3 tubes) across fine-grained sand (FGS), medium-grained sand (MGS), and coarse-grained sand (CGS)

3.3 Thermal Efficiency

Thermal efficiency denotes the system's capacity to transform incoming solar energy into beneficial heat for drying purposes. It denotes the proportion of effective heat gain in the sand bed and product relative to the total solar energy absorbed by the system. This study analyzed the thermal efficiency of fine-grained sand (FGS), medium-grained sand (MGS), and coarse-grained sand (CGS) under one, two, and three evacuated tube collectors (ETC) designs, with measurements conducted until 17:00 hours.

For 1 ETC, thermal efficiency exhibited very high values, with FGS exceeding 180% by 17:00 h. This anomaly arises because, as solar radiation declined in the late afternoon, residual heat stored in the sand bed continued to be released, artificially boosting efficiency values relative to the reduced input. MGS and CGS followed similar trends, reaching ~134% and ~136% respectively. Midday values were relatively stable, with FGS maintaining ~90% efficiency, demonstrating its superior capacity for thermal energy retention (Figure 17). Between 11:00 h and 14:00 h, solar radiation remains relatively constant and at its peak, resulting in stable system efficiency and consistent drying performance. During this period, the dryer effectively converts incoming solar energy into useful heat with minimal fluctuations. Fine-grained sand (FGS) maintains approximately 90% efficiency owing to its superior thermal conductivity and heat storage capacity, which allow it to absorb and retain solar energy efficiently while minimizing heat losses. This stability and high efficiency during peak sunlight hours highlight FGS's strong capability for sustained thermal performance and effective energy utilization in the drying process.

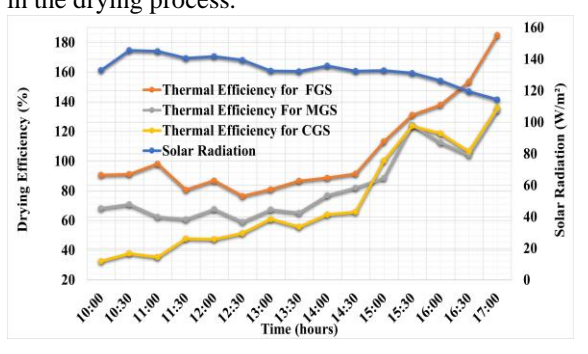


Figure 17. Thermal Efficiency vs. Time for FGS, MGS, and CGS (1 ETC)

Under 2 ETCs, thermal efficiency was comparatively moderate and more stable. Peak values were observed in the late afternoon, with FGS ~146%, MGS ~129%, and CGS ~87%. Across the midday period (11:00–14:00 h), efficiencies ranged between 60–75%, reflecting a balance between solar input and sand-bed heat transfer. The use of two ETCs smoothed variations and minimized sharp fluctuations seen in the single-tube configuration (Figure 18).

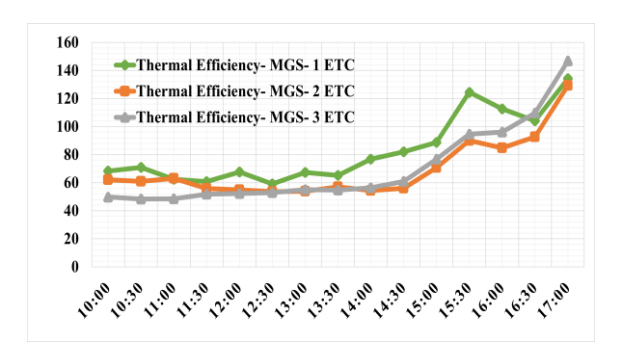


Figure 18. Thermal Efficiency vs. Time for FGS, MGS, and CGS (2 ETCs)

For 3 ETCs, average efficiencies were lower during midday, with FGS ~60–70% and MGS ~50–55%, while CGS ranged ~35–50%. However, similar to other configurations, late afternoon peaks were observed, exceeding 160% for FGS and 139% for CGS. This pattern confirms that higher ETC counts increased instantaneous energy input, but also heightened system losses, reducing stability during periods of peak radiation (Figure 19).

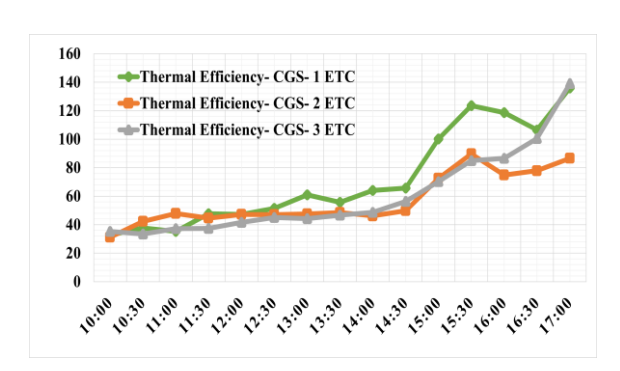


Figure 19. Thermal Efficiency vs. Time for FGS, MGS, and CGS (3 ETCs)

A comparative view of sand-based variation across reveals counts distinct performance characteristics. FGS consistently exhibited the highest thermal efficiencies due to its fine particle which allows more effective thermal conduction and storage. MGS demonstrated balanced but slightly lower values, while CGS performed worst under peak solar inputs but benefited from its thermal inertia in the evening (Figure 20).

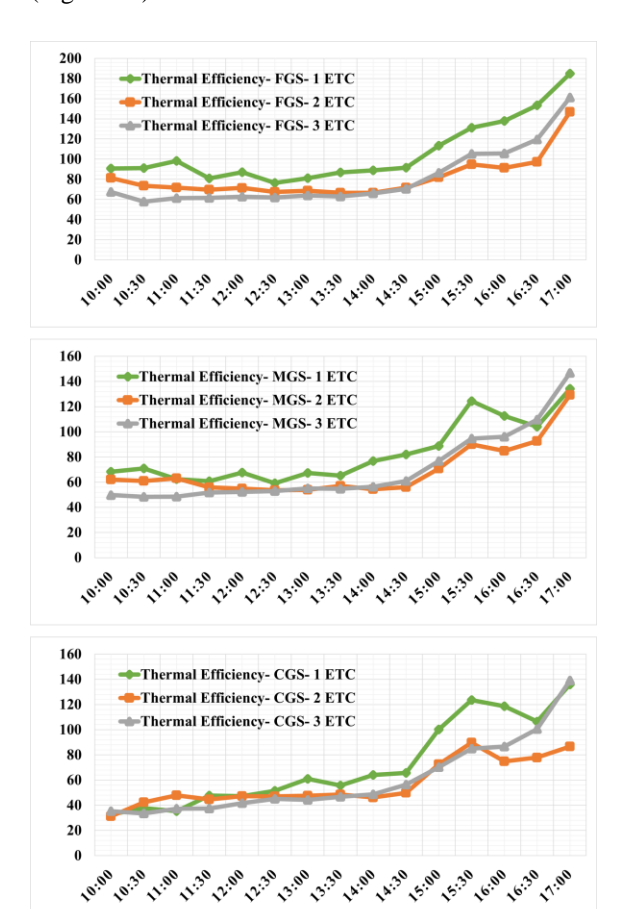


Figure 20. Variation of thermal efficiency with time for different ETC configurations (1, 2, and 3 tubes) across fine-grained sand (FGS), medium-grained sand (MGS), and coarse-grained sand (CGS)

3.4 Decision Matrix for Drying Rate

To identify the most effective configuration, a decision matrix analysis was performed by averaging the drying rate values for each soil type (FGS, MGS, CGS) under different ETC counts (1, 2, and 3). The mean drying rates were normalized on a

0-1 scale to enable direct comparison across all cases

As shown in Figure 21 — Decision Matrix for Drying Rate, the configuration FGS with 3 ETCs achieved the highest normalized score of 1.0, corresponding to a mean drying rate of 0.738 g/min, thereby emerging as the most effective arrangement. This was followed by MGS with 3 ETCs (normalized score: 0.584, mean rate: 0.540 g/min) and FGS with 2 ETCs (normalized score: 0.493, mean rate: 0.497 g/min). The lowest performance was observed for CGS with 1 ETC (normalized score: 0.000, mean rate: 0.262 g/min).

These results clearly demonstrate the strong influence of both collector count and soil texture on drying kinetics. Finer sand fractions (FGS) consistently showed superior performance, benefitting from higher thermal conductivity and improved heat transfer, while coarser fractions (CGS) exhibited slower drying rates due to lower heat retention. Increasing the number of evacuated tube collectors (ETCs) enhances the total solar energy captured and transferred to the drying system, providing greater thermal energy for moisture evaporation. However, the improvement is not linear, as the study observed diminishing returns beyond two collectors—while moving from one to two ETCs significantly increased drying efficiency, adding a third offered only marginal benefits due to thermal and system constraints. Similarly, soil texture plays a vital role in heat transfer performance. Fine-grained sand (FGS), with its higher thermal conductivity, absorbed and retained heat more effectively than medium or coarse sands, resulting in faster and more uniform drying. Overall, optimal drying performance was achieved with two ETCs combined with FGS, balancing energy utilization, system efficiency, and drying rate.

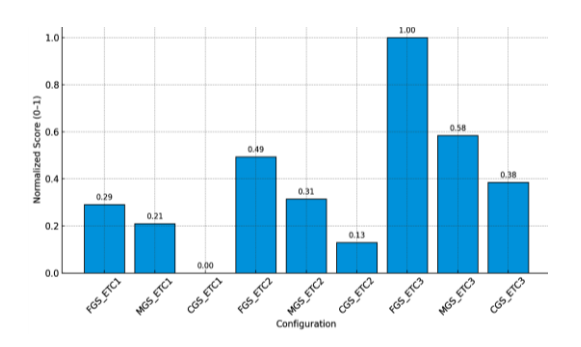


Figure 21. Decision Matrix for Drying Rate

3.5 Visual Validation of Dried Samples

To validate the experimental performance, representative images of the dried carrot samples documented under different operating were conditions. Visual analysis complements the quantitative drying data by showing quality attributes such as color retention, shrinkage, and uniformity.



Figure 22. Visuals of FGS-2 ETC carrot samples

The dried products from the FGS-2 ETC configuration (Figure 22) exhibited bright orange coloration and uniform texture, confirming effective heat transfer and moisture removal. In contrast, the OSD samples (Figure 23) showed noticeable discoloration and uneven drying, highlighting the limitations of open sun exposure.



Figure 23. Visual of OSD carrot samples

4. Conclusion

This study investigated the Solar drying integrated with evacuated tube collectors (ETCs) and sand-based thermal storage provides a sustainable and energy-efficient alternative to conventional fuel-based drying systems.

- The performance of the solar dryer was evaluated for varying numbers of ETCs (1–3) and sand particle sizes—fine-grained (FGS), medium-grained (MGS), and coarse-grained (CGS)—using grated carrot samples.
- The drying rate increased with the number of ETCs, reaching a maximum of 0.93 g/min for the FGS-3 ETC configuration, followed by 0.67 g/min for MGS and 0.57 g/min for CGS under identical conditions.
- Fine-grained sand exhibited superior thermal conductivity, enabling faster moisture removal, while medium- and coarse-grained sands provided more stable drying behavior during later stages.
- Drying efficiency showed an inverse trend with ETC count, decreasing from ~70.7% for FGS—1 ETC to ~20.7% for FGS—3 ETC, indicating a trade-off between enhanced drying rate and energy efficiency.
- Thermal efficiency peaked above 160%, attributed to the residual heat released from the sand-based thermal storage during the post-sunset period.
- The developed system demonstrates significant potential for small-scale agricultural and rural applications, offering an economical and ecofriendly solution for drying fruits, vegetables, and other perishable products.

5. Practical Implications

The present study contributes to the growing body of research on solar drying systems by introducing an innovative integration of sand-based thermal storage with evacuated tube collector (ETC)-assisted drying. Unlike conventional solar dryers that rely solely on direct solar radiation or air heating. configuration utilizes the high thermal capacity of sand as a latent heat storage medium, enabling extended drying operation even during low solar intensity periods. The combination of sand-based storage and ETCs enhances both the thermal stability and heat transfer efficiency, ensuring more consistent drying conditions and improved product quality. A major contribution of this work lies in the systematic analysis of sand particle size (fine, medium, coarse), ETC count (1-3) to establish their interdependent effects on drying rate and efficiency. The study provides quantitative insights into the trade-off between faster drying and overall thermal efficiency, offering valuable data for system optimization. These findings can inform the design

and scaling of solar dryers tailored for different climatic conditions and crop types. In terms of practical applications, the proposed solar dryer holds significant potential for small-scale agricultural use in rural and semi-urban regions, where access to electricity or conventional fuel sources is limited. By utilizing locally available materials such as sand and low-cost ETC units, the system provides an economical and environmentally sustainable solution for food preservation. It can be effectively employed for drying fruits, vegetables, and grains, helping to reduce post-harvest losses and enhance food security. Furthermore, the approach aligns with global sustainability goals by minimizing carbon emissions and promoting renewable energy utilization in agricultural processing.

6. Future Scope

- Future work can explore the integration of hybrid energy sources, such as photovoltaic-thermal (PV/T) units or biomass-assisted systems, to ensure continuous drying during cloudy or nighttime conditions.
- Computational fluid dynamics (CFD) and AIbased optimization models can be employed to analyze airflow, temperature distribution, and moisture diffusion for improved dryer design.
- Investigation of alternative thermal storage materials, including phase change materials (PCMs), hybrid sand–PCM mixtures, or locally available natural materials, can enhance heat storage capacity and stability.
- Development of automated control systems for monitoring and regulating air temperature, humidity, and flow rate can improve drying efficiency and product quality.
- Scaling and customization of the solar dryer for various crops and climatic zones can expand its applicability to diverse agricultural settings.
- Conducting economic feasibility studies and life-cycle assessments (LCA) can help evaluate the long-term sustainability and environmental benefits of the system.
- Field trials and pilot-scale demonstrations are recommended to validate laboratory findings under real-world conditions and assess practical performance.
- Promotion of technology transfer and training programs for small-scale farmers can support rural development, enhance food preservation, and encourage adoption of renewable energybased drying systems.

Nomenclature	
C_p	Specific heat capacity, J/kg·K
CGS	Coarse-grained size
D_R	Drying rate, g/min
ETC	Evacuated tube collector
FGS	Fine-grained size
I	Solar radiation intensity, W/m²
m_a	Air mass flow rate, kg/s
MC_{db}	Moisture content, % (dry basis)
MC_{wb}	Moisture content, % (wet basis)
MGS	Medium-grained size
MR	Moisture ratio
t	Drying time, min
T_{ch}	Drying chamber temperature, °C
T_s	Sand bed temperature, °C
η_d	Drying efficiency, %
$oldsymbol{\eta}_{th}$	Thermal efficiency, %

References

- [1] D. Benmenine, E. El-Bialy, D. Belatrache, A. Benmenine, and S. M. Shalaby, "Experimental investigation of a direct solar dryer equipped with parabolic-trough solar concentrator for drying Moringa leaves in the region of Algerian sahara, Ouargla city," *J. Atmos. Solar-Terrestrial Phys.*, vol. 274, no. March, p. 106595, 2025, doi: 10.1016/j.jastp.2025.106595.
- [2] A. P. Singh, A. Gupta, A. Biswas, and B. Das, "Experimental study of a novel photovoltaic-thermal-thermoelectric generator-based solar dryer for grapes drying," *Int. J. Green Energy*, vol. 21, no. 5, pp. 1161–1173, 2024, doi: 10.1080/15435075.2023.2244046.
- [3] N. Kalita, P. Muthukumar, and A. Dalal, "Performance investigation of a hybrid solar dryer with electric and biogas backup air heaters for chilli drying," *Therm. Sci. Eng. Prog.*, vol. 52, no. April, p. 102646, 2024, doi: 10.1016/j.tsep.2024.102646.
- [4] G. G. Radhakrishnan, M. Sattanathan, R. K. G. Radhakrishnan, and A. K. Jeevan, "Phase-change material-based solar dryer:

- An experimental investigation for drying mango pulp," *Sol. Energy*, vol. 277, no. March, p. 112716, 2024, doi: 10.1016/j.solener.2024.112716.
- [5] S. Suherman, D. D. Anggoro, S. Sugiharto, and M. A. Asy-Syaqiq, "Investigation of a mixed-mode solar dryer assisted with an air recycling system and phase change material unit for coffee beans drying: An experimental study," *Renew. Energy*, vol. 254, no. June, p. 123762, 2025, doi: 10.1016/j.renene.2025.123762.
- [6] M. Mokhtarian, A. Kalbasi-Ashtari, and H. W. Xiao, "Effects of solar drying operation equipped with a finned and double-pass heat collector on energy utilization, essential oil extraction and bio-active compounds of peppermint (Mentha Piperita L.)," *Dry. Technol.*, vol. 40, no. 5, pp. 897–923, 2022, doi: 10.1080/07373937.2020.1836650.
- [7] C. N. Deepak and A. K. Behura, "Experimental analysis of a mixed mode solar tunnel dryer for drying tomato: Energy, exergy and environmental assessment," *Therm. Sci. Eng. Prog.*, vol. 63, no. June 2024, p. 103707, 2025, doi: 10.1016/j.tsep.2025.103707.
- [8] B. Das, P. Singh, and P. Kalita, "Performance Evaluation of a Mixed-Mode solar dryer with PCM-based energy storage for efficient drying of Baccaurea ramiflora," *Sol. Energy*, vol. 288, no. January, p. 113279, 2025, doi: 10.1016/j.solener.2025.113279.
- [9] M. U. H. Suzihaque and R. Driscoll, "Effects of Solar Radiation, Buoyancy of Air Flow and Optimization Study of Coffee Drying in a Heat Recovery Dryer," *Procedia Eng.*, vol. 148, pp. 812–822, 2016, doi: 10.1016/j.proeng.2016.06.617.
- [10] N. Arbaoui *et al.*, "Impact of a solar greenhouse converted into a solar dryer on the performance indicators (energy efficiency, bio-chemical, economic and environmental) during summer season," *Sol. Energy*, vol. 291, no. March, p. 113416, 2025, doi: 10.1016/j.solener.2025.113416.
- [11] Y. Luo *et al.*, "ur na l P of," *Carbohydr. Polym.*, p. 115713, 2019, doi: 10.1016/j.csite.2025.106786.
- [12] V. Joseph *et al.*, "An innovative method based on CFD to simulate the influence of photovoltaic panels on the microclimate in agrivoltaic conditions," *Sol. Energy*, vol.

- 297, no. May, p. 113571, 2025, doi: 10.1016/j.solener.2025.113571.
- [13] H. Dadhaneeya, P. K. Nema, V. K. Arora, S. B. Kokane, and K. R. Pawar, "Smart nextgen drying solution: A study of design, development and performance evaluation of IoT-enabled IR-assisted refractance window dryer," *Dry. Technol.*, vol. 42, no. 15, pp. 2212–2231, 2024, doi: 10.1080/07373937.2024.2415422.
- [14] M. Aktaş, A. Khanlari, B. Aktekeli, and A. Amini, "Analysis of a new drying chamber for heat pump mint leaves dryer," *Int. J. Hydrogen Energy*, vol. 42, no. 28, pp. 18034–18044, 2017, doi: 10.1016/j.ijhydene.2017.03.007.
- [15] S. Srivastava and A. Yadav, "Economic analysis of water production from atmospheric air using Scheffler reflector," *Appl. Water Sci.*, vol. 9, no. 1, pp. 1–10, 2019, doi: 10.1007/s13201-018-0883-7.
- [16] P. Qu, M. Zhang, A. S. Mujumdar, and D. Yu, "Efficient drying of laser-treated raspberry in a pulse-spouted microwave freeze dryer," *Dry. Technol.*, vol. 40, no. 12, pp. 2433–2444, 2022, doi: 10.1080/07373937.2022.2058959.
- [17] G. N. Abdel-Rahman, E. M. Saleh, A. Hegazy, A. S. M. Fouzy, and M. A. Embaby, "Safety improvement of the open sun dried Egyptian Siwi dates using closed solar dryer," *Heliyon*, vol. 9, no. 11, p. e22425, 2023, doi: 10.1016/j.heliyon.2023.e22425.
- [18] E. Hürdoğan, K. N. Çerçi, D. B. Saydam, and C. Ozalp, "Experimental and Modeling Study of Peanut Drying in a Solar Dryer with a Novel Type of a Drying Chamber," *Energy Sources, Part A Recover. Util. Environ. Eff.*, vol. 44, no. 2, pp. 5586–5609, 2022, doi: 10.1080/15567036.2021.1974126.
- [19] V. M. Swami, A. T. Autee, and A. T R, "Experimental analysis of solar fish dryer using phase change material," *J. Energy Storage*, vol. 20, no. 669, pp. 310–315, 2018, doi: 10.1016/j.est.2018.09.016.
- [20] M. C. Ndukwu *et al.*, "Drying kinetics and thermo-economic analysis of drying hot water blanched ginger rhizomes in a hybrid composite solar dryer with heat exchanger," *Heliyon*, vol. 9, no. 2, p. e13606, 2023, doi: 10.1016/j.heliyon.2023.e13606.
- [21] R. J. Mongi and S. J. Ngoma, "Effect of

- Solar Drying Methods on Proximate Composition, Sugar Profile and Organic Acids of Mango Varieties in Tanzania," *Appl. Food Res.*, vol. 2, no. 2, 2022, doi: 10.1016/j.afres.2022.100140.
- [22] S. Ghafari and M. Behzad, "Enhancing solar dryer performance with combined flat plate absorber and parabolic trough collector: A comprehensive techno-economic and environmental study ★," Sustain. Energy Technol. Assessments, vol. 82, no. June 2024, p. 104486, 2025, doi: 10.1016/j.seta.2025.104486.
- P. Ganesan and T. M. Eikevik, "Current [23] scientific progress in solar-assisted vapor heat compression pump technology: Advanced design and configuration, refrigerant, performance, economic environmental assessments," Thermofluids, vol. 23, no. July, p. 100783, 2024, doi: 10.1016/j.ijft.2024.100783.
- [24] A. K. Hussein, "Applications of nanotechnology in renewable energies—A comprehensive overview and understanding". *Renewable and Sustainable Energy Reviews*, 42, pp.460-476,2015, doi:10.1016/j.rser.2014.10.027.
- [25] A.K. Hussein, A. Walunj, and L. Kolsi, "Applications of nanotechnology to enhance the performance of the direct absorption solar collectors". *Journal of Thermal Engineering*, 2(1), pp.529-540, 2016, doi: 10.18186/jte.46009.
- [26] A. K. Hussein, "Applications of nanotechnology to improve the performance of solar collectors—Recent advances and overview". *Renewable and Sustainable Energy Reviews*, 62, pp.767-792, 2016, doi: 10.1016/j.rser.2016.04.050.
- [27] A. K. Hussein, D. Li, L. Kolsi, S. Kata, and B. Sahoo, "A review of nano fluid role to improve the performance of the heat pipe solar collectors". *Energy Procedia*, 109, pp.417-424, 2017, doi: 10.1016/j.energy.2021.122794.
- [28] N. Hashemian, and A. Noorpoor, "Thermoeco-environmental investigation of a newly developed solar/wind powered multigeneration plant with hydrogen and ammonia production options". *Journal of Solar Energy Research*, 8(4), pp.1728-1737, 2023, doi: 10.22059/jser.2024.374028.1388.
- [29] N. Hashemian, and A. Noorpoor,

- "Assessment and multi-criteria optimization of a solar and biomass-based multi-generation system: Thermodynamic, exergoeconomic and exergoenvironmental aspects". *Energy conversion and management*, 195, pp.788-797, 2019, doi: 10.1016/j.enconman.2019.05.039.
- [30] S. Suherman, M. A. Asy-Syaqiq, F. A. Rosyid, A. R. Nugroho, A. H. Marpaung, and B. W. H. E. Prasetiyono, "Effect of loading capacity on drying characteristics and techno-economic analysis of maize kernels dried using a large-scale greenhouse solar dryer," *Therm. Sci. Eng. Prog.*, vol. 65, no. July, 2025, doi: 10.1016/j.tsep.2025.103914.
- [31] M. C. Gilago, V. R. Mugi, and C. V. P., "Performance assessment of passive indirect solar dryer comparing without and with heat storage unit by investigating the drying kinetics of carrot," *Energy Nexus*, vol. 9, no. November 2022, p. 100178, 2023, doi: 10.1016/j.nexus.2023.100178.
- [32] M. C. Gilago, V. R. Mugi, and V. P. Chandramohan, "Evaluation of drying kinetics of carrot and thermal characteristics of natural and forced convection indirect solar dryer," *Results Eng.*, vol. 18, no. April, p. 101196, 2023, doi: 10.1016/j.rineng.2023.101196.
- [33] V. V. Tyagi *et al.*, "Sustainable growth of solar drying technologies: Advancing the use of thermal energy storage for domestic and industrial applications," *J. Energy Storage*, vol. 99, no. August, 2024, doi: 10.1016/j.est.2024.113320.
- [34] M. N. Musembi, K. S. Kiptoo, and N. Yuichi, "Design and Analysis of Solar Dryer for Mid-Latitude Region," *Energy Procedia*, vol. 100, no. September, pp. 98–110, 2016, doi: 10.1016/j.egypro.2016.10.145.
- [35] R. Umayal Sundari and E. A. Veeramanipriya, "Performance evaluation, morphological properties and drying kinetics of untreated Carica Papaya using solar hybrid dryer integrated with heat storage material," J. Energy Storage, vol. 55, no. PC. p. 105679, 2022. doi: 10.1016/j.est.2022.105679.
- [36] V. S. Krishna, S. K. Jain, N. L. Panwar, and R. Sree, "An overview on Phase Change Material incorporated in convective solar dryers," *J. Energy Storage*, vol. 131, no. PA, p. 117486, 2025, doi:

- 10.1016/j.est.2025.117486.
- [37] J. P. Ekka and M. Palanisamy, "Determination of heat transfer coefficients and drying kinetics of red chilli dried in a forced convection mixed mode solar dryer," *Therm. Sci. Eng. Prog.*, vol. 19, no. January, p. 100607, 2020, doi: 10.1016/j.tsep.2020.100607.
- [38] S. Tiwari, G. N. Tiwari, and I. M. Al-Helal, "Development and recent trends in greenhouse dryer: A review," *Renew. Sustain. Energy Rev.*, vol. 65, pp. 1048–1064, 2016, doi: 10.1016/j.rser.2016.07.070.
- [39] P. Sukkanta, K. Eiamkij, N. Junset, and K. Mongkoldhumrongkul, "Oyster mushroom drying efficiency using a solar dryer," *Energy Reports*, vol. 9, pp. 479–486, 2023, doi: 10.1016/j.egyr.2023.01.062.
- [40] S. Vijayan, T. V. Arjunan, and A. Kumar, "Mathematical modeling and performance analysis of thin layer drying of bitter gourd in sensible storage based indirect solar dryer," *Innov. Food Sci. Emerg. Technol.*, vol. 36, pp. 59–67, 2016, doi: 10.1016/j.ifset.2016.05.014.
- [41] G. P. Arul, S. Shanmugam, A. R. Veerappan, and P. Kumar, "Mathematical modeling and experimental studies on a dual inclined oscillating bed with double pass solar dryer for drying of non parboiled paddy grains," *Energy Sources, Part A Recover. Util. Environ. Eff.*, vol. 43, no. 22, pp. 2935–2946, 2021, doi: 10.1080/15567036.2019.1670754.
- [42] F. Chabane, N. Moummi, and A. Brima, "An experimental study and mathematical modeling of solar drying of moisture content of the mint, apricot, and green pepper," *Energy Sources, Part A Recover. Util. Environ. Eff.*, vol. 45, no. 2, pp. 4697–4711, 2023, doi: 10.1080/15567036.2019.1670755.
- [43] R. Kumar, S. V. M. Navaneethakrishnan, and S. Solaiachari, "Hybrid glass-carbon fiber composites for solar greenhouse dryer trays: a 3D computational analysis," *Adv. Compos. Mater.*, vol. 00, no. 00, pp. 1–22, 2024, doi: 10.1080/09243046.2024.2365474.
- [44] S. Shoeibi *et al.*, "Recent advancements in applications of encapsulated phase change materials for solar energy systems: A state of the art review," *J. Energy Storage*, vol. 94, no. June, p. 112401, 2024, doi:

- 10.1016/j.est.2024.112401.
- [45] S. M. Shalaby, M. A. Bek, and A. A. El-Sebaii, "Solar dryers with PCM as energy storage medium: A review," *Renew. Sustain. Energy Rev.*, vol. 33, pp. 110–116, 2014, doi: 10.1016/j.rser.2014.01.073.